CHAPTER 14

Impact of climate change mitigation on ocean acidification projections

Fortunat Joos, Thomas L. Frölicher, Marco Steinacher, and Gian-Kasper Plattner

14.1   Introduction

Ocean acidification caused by the uptake of carbon dioxide (CO_2) by the ocean is an important global change problem (Kleypas *et al.* 1999; Caldeira and Wickett 2003; Doney *et al.* 2009). Ongoing ocean acidification is closely linked to global warming, as acidification and warming are primarily caused by continued anthropogenic emissions of CO_2 from fossil fuel burning (Marland *et al.* 2008), land use, and land-use change (Strassmann *et al.* 2007). Future ocean acidification will be determined by past and future emissions of CO_2 and their redistribution within the earth system and the ocean. Calculation of the potential range of ocean acidification requires consideration of both a plausible range of emissions scenarios and uncertainties in earth system responses, preferably by using results from multiple scenarios and models.

The goal of this chapter is to map out the spatio-temporal evolution of ocean acidification for different metrics and for a wide range of multigas climate change emissions scenarios from the integrated assessment models (Nakićenović 2000; Van Vuuren *et al.* 2008b). By including emissions reduction scenarios that are among the most stringent in the current literature, this chapter explores the potential benefits of climate mitigation actions in terms of how much ocean acidification can be avoided and how much is likely to remain as a result of inertia within the energy and climate systems. The long-term impacts of carbon emissions are addressed using so-called zero-emissions commitment scenarios and pathways leading to stabilization of atmospheric CO_2. Discussion will primarily rely on results from the cost-efficient Bern2.5CC model (Plattner

et al. 2008) and the comprehensive carbon cycle–climate model of the National Centre for Atmospheric Research (NCAR), CSM1.4-carbon (Steinacher *et al.* 2009; Frölicher and Joos 2010).

The magnitude of the human perturbation of the climate system is well documented by observations (Solomon *et al.* 2007). Carbon emissions from human activities force the atmospheric composition, climate, and the geochemical state of the ocean towards conditions that are unique for at least the last million years (see Chapter 2). The current atmospheric CO_2 concentration of 390 ppmv is well above the natural range of 172 to 300 ppmv of the past 800 000 years (Lüthi *et al.* 2008). The rate of increase in CO_2 and in the radiative forcing from the combination of the well-mixed greenhouse gases CO_2, methane (CH_4), and nitrous oxide (N_2O) is larger during the Industrial Era than during any comparable period of at least the past 16 000 years (Joos and Spahni 2008). Ocean measurements over recent decades show that the increase in surface-ocean CO_2 is being paralleled by a decrease in pH (Doney *et al.* 2009). Ongoing global warming is unequivocal (Solomon *et al.* 2007): observational data show that global-mean sea level is rising, ocean heat content increasing, Arctic sea ice retreating, atmospheric water vapour content increasing, and precipitation patterns changing. The last decade (2000 to 2009) was, on a global average, the warmest in the instrumental record (http://data.giss.nasa.gov/gistemp/). Proxy reconstructions suggest that recent anthropogenic influences have widened the last-millennium multidecadal temperature range by 75% and that late 20th century warmth exceeded peak temperatures over the past millennium by 0.3°C (Frank *et al.* 2010).

The range of plausible 21st century emissions pathways leads to further global warming and ocean acidification (Van Vuuren *et al.* 2008b; Strassmann *et al.* 2009). Projections based on the scenarios of the Special Report on Emissions Scenarios (SRES) of the Intergovernmental Panel on Climate Change (IPCC) give reductions in average global surface pH of between 0.14 and 0.35 units over the 21st century, adding to the present decrease of 0.1 units since pre-industrial time (Orr *et al.* 2005; see also Chapters 1 and 3). Comprehensive earth system model simulations show that continued carbon emissions over the 21st century will cause irreversible climate change on centennial to millennial timescales in most regions, and impacts related to ocean acidification and sea level rise will continue to aggravate for centuries even if emissions are stopped by the year 2100 (Frölicher and Joos 2010). In contrast, in the absence of future anthropogenic emissions of CO_2 and other radiative agents, forced changes in surface temperature and precipitation will become smaller in the next centuries than internal variability for most land and ocean grid cells and ocean acidification will remain limited. This demonstrates that effective measures to reduce anthropogenic emissions can make a difference. However, continued carbon emissions will affect climate and the ocean over the next millennium and beyond (Archer *et al.* 1999; Plattner *et al.* 2008) and related climate and biogeochemical impacts pose a substantial threat to human society.

Thirty years ago, with their box-diffusion carbon cycle model, Siegenthaler and Oeschger (1978) demonstrated the long lifetime of an atmospheric CO_2 perturbation and pointed out that carbon emissions must be reduced 'if the atmospheric radiation balance is not to be disturbed in a dangerous way'. The United Nations Framework Convention on Climate Change (UNFCCC) that came into force in 1994 has the ultimate objective (article 2) 'to achieve . . . stabilization of greenhouse gas concentrations in the atmosphere at a level that would prevent dangerous anthropogenic interference with the climate system. Such a level should be achieved within a time frame sufficient to allow ecosystems to adapt naturally to climate change...' (UN 1992). Scenarios provide a useful framework for establishing policy-relevant information related to the UNFCCC. Here, the link between atmospheric CO_2 level and ocean acidification, and the timescales of change, are addressed.

The outline of this chapter is as follows. In the next section, we will discuss different classes of scenarios, their underlying assumptions, and how these scenarios are used. Metrics for assessing ocean acidification are also introduced. In Section 14.3, the evolution over this century of atmospheric CO_2, global-mean surface air temperature, and global-mean surface ocean acidification for the recent range of baseline and mitigation scenarios from integrated assessment models is presented. In Section 14.4, the minimum commitment, as a result of past and 21st century emissions, to long-term climate change and ocean acidification arising from inertia in the earth system alone is addressed. In Section 14.5, regional changes in surface ocean chemistry are discussed. In Section 14.6, delayed responses, irreversibility, and changes in the deep ocean are addressed using results from the comprehensive NCAR CSM1.4-carbon model. Finally, in Section 14.7, idealized profiles leading to CO_2 stabilization are discussed to further highlight the link between greenhouse gas stabilization, climate change, and ocean acidification. The overarching logic is to use the cost-efficient Bern2.5CC model to explore the scenario space and uncertainties for global-mean values and the NCAR CSM1.4-carbon model to investigate regional details for a limited set of scenarios. The set of baseline and emissions scenarios and associated changes in CO_2 and global-mean surface temperature have been previously discussed (Van Vuuren *et al.* 2008b; Strassmann *et al.* 2009). We also refer to the literature for a more detailed discussion of the NCAR CSM1.4-carbon ocean acidification results (Steinacher *et al.* 2009; Frölicher and Joos 2010).

14.2 Scenarios and metrics

Scenario-based projections are a scientific tool kit for investigating alternative evolutions of anthropogenic emissions and their influence on climate, the earth system, and the socio-economic system. Scenario-based projections are not to be misunderstood as predictions of the future, and as the time horizon increases the basis for the underlying assumptions becomes increasingly uncertain.

One class of scenarios includes idealized emissions or concentration pathways to investigate processes, feedbacks, timescales, and inertia in the climate system. These scenarios are usually developed from a natural science perspective and used for their illustrative power. Examples are a complete instantaneous reduction of emissions at a given year or idealized pathways leading to stabilization of greenhouse gas concentrations (Schimel *et al.* 1997). Another class of emissions scenarios has been developed using integrated assessment frameworks and integrated assessment models (IAMs) by considering plausible future demographic, social, economic, technological, and environmental developments. Examples include the scenarios of the IPCC SRES (Nakićenović *et al.* 2000) and the more recently developed representative concentration pathways (RCPs; Moss *et al.* 2008, 2010; Van Vuuren *et al.* 2008a).

The SRES emissions scenarios do not include explicit climate change mitigation actions. Such scenarios are usually called baseline or reference scenarios. In this chapter, results based on the two illustrative SRES scenarios B1 and A2, a low- and a high-emissions baseline scenario, are discussed (Fig. 14.1). The SRES scenarios have been widely used in the literature and in the IPCC Fourth Assessment Report. They are internally consistent scenarios in the sense that each is based on a 'narrative storyline' that describes the relationships between the forces driving emissions. The 21st century emissions of the major anthropogenic greenhouse gases [CO_2, CH_4, N_2O, halocarbons, and sulphur hexafluoride (SF_6)], aerosols and tropospheric ozone precursors [sulphur dioxide (SO_2), carbon monoxide (CO), NO_x, and volatile organic compounds (VOCs)] are quantified with IAMs. The extent of the technological improvements contained in the SRES scenarios is not always appreciated. The SRES scenarios include already large and important improvements in energy intensity (energy used per unit of gross domestic product) and the deployment of non-carbon-emitting energy supply technologies compared with the present (Edmonds *et al.* 2004). By the year 2100, the primary energy demand in the SRES scenarios ranges from 55% to more than 90% lower than had no improvement in energy intensity occurred. In addition, in many of the SRES scenarios the deployment of non-carbon-emitting energy supply systems (solar, wind, nuclear, and biomass) exceeds the size of the global energy system in 1990.
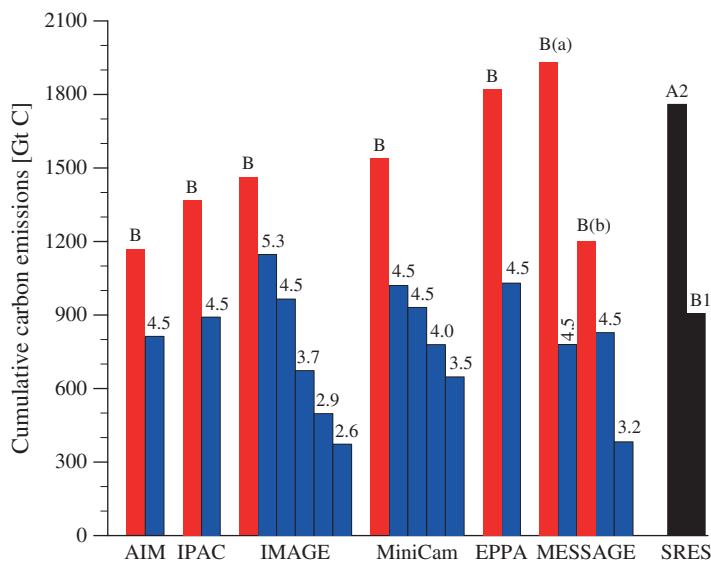
Figure 14.1 Cumulative CO_2 emissions in gigatonnes of carbon (Gt C) over the 21st century for a range of baseline (B; red), climate mitigation (blue), and the SRES A2 and B1 (black) scenarios. The numbers related to the mitigation scenarios indicate the radiative forcing targets in W m^{-2} imposed in the IAMs. The labels below the columns refer to the IAMs used to quantify the scenarios (Weyant *et al.* 2006) and to the SRES scenarios (Nakićenović 2000), respectively.

However, by design they do not include explicit policies to mitigate greenhouse gas emissions, which would lower the extent of climate change experienced over the 21st century.

Progress in developing multigas mitigation scenarios after the SRES report now allows for a comparison between consequences for the earth system of climate mitigation versus baseline scenarios. Figure 14.1 illustrates the relationship between scenarios and individual IAMs and how individual mitigation scenarios are linked to a specific baseline scenario for the post-SRES set of scenarios. Many mitigation scenarios were generated with several IAMs as part of the Energy Modeling Forum Project 21 (EMF-21; Weyant *et al.* 2006). The IAMs feature representations of the energy system and other parts of the economy, such as trade and agriculture, with varying levels of spatial and process detail. They also include formulations to translate emissions into concentrations and the associated radiative forcing (RF). The latter is a metric for the perturbation of the radiative balance of the lower atmosphere–surface system. Scenarios are generated by minimizing the total costs under the constraints set by societal drivers (e.g. population, welfare, and technological innovation) and most are related to SRES 'storylines'. Adding a constraint on RF in a baseline scenario leads to a scenario with policies specifically aimed at mitigation. The mitigation scenarios analysed here are constrained by stabilization of total RF in the period 2100 to 2150 with RF targets ranging from 2.6 to 5.3 W m^{-2}. From the wider set of baseline and mitigation scenarios described in the literature, four have been specifically selected and termed representative concentration pathways (RCPs). These include two mitigation scenarios with a RF target of 2.6 and 4.5 W m^{-2} and two baseline scenarios with a RF of around 6 and 8.5 W m^{-2} by the end of this century.

Two metrics appear particularly well suited for characterizing the outcome of a scenario in terms of ocean acidification. These are changes in pH and changes in the saturation state of water with respect to aragonite, a mineral form of calcium carbonate ($CaCO_3$) secreted by marine organisms. Ocean uptake of the weak acid CO_2 from the atmosphere causes a reduction in pH and in turn alters the $CaCO_3$ precipitation equilibrium (see Chapter 1).

Recent studies indicate that ocean acidification due to the uptake of CO_2 has adverse consequences for many marine organisms as a result of decreased $CaCO_3$ saturation, affecting calcification rates, and via disturbance to acid–base physiology (see Chapters 6–8). Vulnerable organisms that build shells and other structures of $CaCO_3$ in the relatively soluble form of aragonite or high-magnesian calcite, but also organisms that form $CaCO_3$ in the more stable form of calcite may be affected. Undersaturation as projected for the high-latitude ocean (Orr *et al.* 2005; Steinacher *et al.* 2009) has been found to affect pteropods for example, an abundant group of species forming aragonite shells (Orr *et al.* 2005; Comeau *et al.* 2009). Changes in $CaCO_3$ saturation are also thought to affect coral reefs (Kleypas *et al.* 1999; Langdon and Atkinson 2005; Hoegh-Guldberg *et al.* 2007; Cohen and Holcomb 2009). The impacts are probably not restricted to ecosystems at the ocean surface, but potentially also affect life in the deep ocean such as the extended deep-water coral systems and ecosystems at the ocean floor. The degree of sensitivity varies among species (Langer *et al.* 2006; Müller *et al.* 2010) and there is a debate about whether some taxa may show enhanced calcification at the levels of CO_2 projected to occur over the 21st century (Iglesias-Rodriguez *et al.* 2008). This wide range of different responses is expected to affect competition among species, ecosystem structure, and overall community production of organic material and $CaCO_3$. On the other hand, the impact of plausible changes in $CaCO_3$ production and export (Gangstø *et al.* 2008) on atmospheric CO_2 is estimated to be small (Heinze 2004; Gehlen *et al.* 2007). Other impacts of ocean acidification with potential influences on marine ecosystems include alteration in the speciation of trace metals as well as an increase in the transparency of the ocean to sound (Hester *et al.* 2008). The changes in the chemical composition of seawater such as higher concentrations of dissolved CO_2 are also likely to affect the coupled carbon and nitrogen cycle and the food web in profound ways (Hutchins *et al.* 2009), and the volume of water with a ratio of oxygen to CO_2 below the threshold for aerobic life is likely to expand (Brewer and Peltzer 2009).

The saturation state with respect to aragonite, Ω_a, is defined by:

$$\Omega_a = \frac{[Ca^{2+}][CO_3^{2-}]}{K_{sp}^*}$$

where brackets denote concentrations in seawater, here for calcium ions and carbonate ions, and K_{sp}^* is the apparent solubility product defined by the equilibrium relationship for the dissolution reaction of aragonite. Similarly, saturation can be defined with respect to calcite which is less soluble than aragonite. Uptake of CO_2 causes an increase in total dissolved inorganic carbon (C_T) and a decrease in the carbonate ion concentration and in saturation (see Chapter 1). Shells or other structures start to dissolve in the absence of protective mechanisms when saturation falls below 1 for the appropriate mineral phase. A value of Ω greater than 1 corresponds to supersaturation. Supersaturated conditions are possible, as the activation energy for forming aragonite or calcite is high.

The pH describes the concentration or, more precisely, the activity of the hydrogen ion in water, $a_{H'}$ by a logarithmic function:

$$pH_T = -\log_{10} a_{H^+}.$$

The activity of hydrogen ion is important for all acid–base reactions. In this chapter, the total pH scale is used as indicated by the subscript T.

14.3 Baseline and mitigation emissions scenarios for the 21st century: how much acidification can be avoided?

Figure 14.1 shows the cumulative carbon emissions over this century for the recent set of baseline and mitigation scenarios (Van Vuuren *et al.* 2008b) and Fig. 14.2 their temporal evolution. Cumulative CO_2 emissions are in the range of 1170 to 1930 Gt C for the seven baseline scenarios and between 370 and 1140 Gt C for the mitigation scenarios, with the highest emissions associated with a high forcing and a weak mitigation target. In the baseline (no climate policy) scenarios, the range of increase in greenhouse gas emissions by 2100 is from 70 to almost 250% compared with the year 2000 (here, emissions are measured in CO_2-equivalent—CO_2-equivalent emissions of a forcing agent denote the amount of CO_2 emissions that would cause the same radiative forcing over a time period of 100 years; IPCC 2007). Emissions growth slows down in the second half of the century in all baseline scenarios, because of a combination of stabilizing global population levels and continued technological change. The mitigation scenarios necessarily follow a different path, with a peak in global emissions between 2020 and 2040 at a maximum value of 50% above current emissions.

The projected CO_2 concentrations for the baseline cases calculated with the Bern2.5CC model (Plattner *et al.* 2008) range from 650 to 960 ppmv in 2100 using best-estimate model parameters (Fig. 14.2C). The CO_2 concentrations in the mitigation scenarios range from 400 to 620 ppmv in 2100. Uncertainties in the carbon cycle and climate sensitivity increase the overall range to 370 to 1310 ppmv (bars in Fig. 14.2C; Plattner *et al.* 2008). Uncertainties are particularly large for the high end. The two scenario sets, baseline and mitigation, are also distinct with respect to their trends. All baseline scenarios show an increasing trend in atmospheric CO_2, implying rising concentrations beyond 2100. In contrast, the mitigation scenarios show little growth or even a declining trend in CO_2 by 2100.

Projected global-mean surface air temperature changes by the year 2100 (relative to 2000) are 2.4 to 4.2°C (Fig. 14.2D) for the baseline scenarios and best-estimate Bern2.5CC model parameters. Uncertainties in the carbon cycle and climate sensitivity more than double the ranges associated with emissions. For the mitigation scenarios, the projected temperature changes by 2100 are 1.1 to 2.1°C using central model parameters. The mitigation scenarios bring down the overall range of CO_2 and temperature change substantially relative to the baseline range. As for CO_2, the greatest difference compared with the baseline is seen during the second part of the century, when the rate of temperature change slows considerably in all mitigation scenarios in contrast to the baseline scenarios. In several mitigation scenarios, surface air temperature has more or less stabilized by year 2100 (Van Vuuren *et al.* 2008b; Strassmann *et al.* 2009).

The evolution of the global-mean saturation state of aragonite (Fig. 14.2E) and pH_T (Fig. 14.2F) in the surface ocean mirrors the evolution of atmospheric
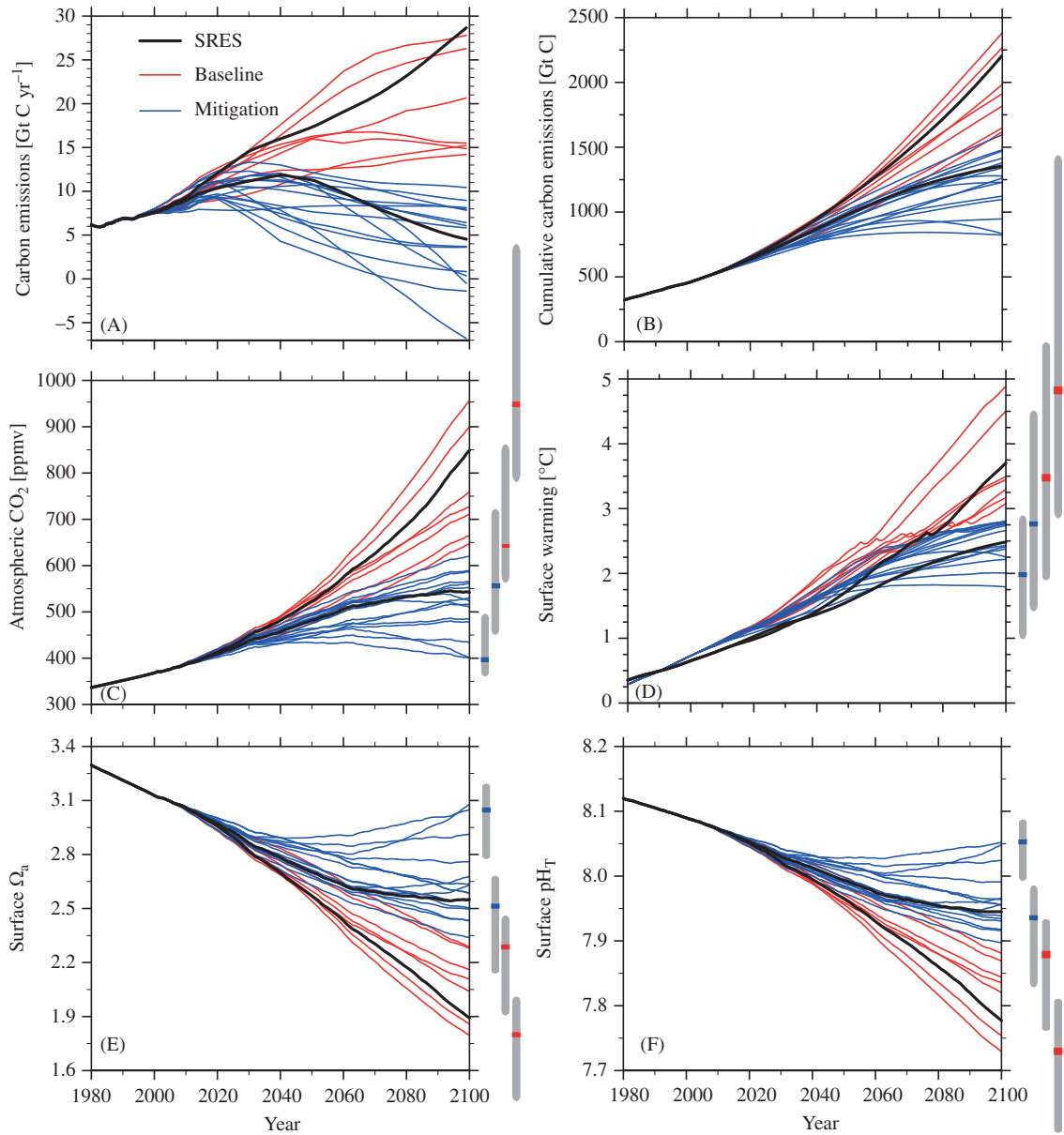
Figure 14.2   (A) Annual and (B) cumulative CO_2 emissions prescribed in the Bern2.5CC model and projected (C) atmospheric CO_2, (D) changes in global-mean surface air temperature, (E) global average surface saturation with respect to $CaCO_3$ in the form of aragonite, and (F) global average surface pH on the total pH scale (pH_T). Baseline scenarios are shown by red lines and mitigation scenarios by blue dotted lines. The SRES high-emissions A2 and low-emissions B1 marker scenarios are given by black lines. Bars indicate uncertainty ranges for the year 2100 and for the four representative concentration pathways (RCPs), marked for evaluation by climate modellers in preparation for the IPCC Fifth Assessment Report. The ranges were obtained by combining different assumptions about the behaviour of the CO_2 fertilization effect on land, the response of soil heterotrophic respiration to temperature, and the turnover time of the ocean, thus approaching an upper boundary of uncertainties in the carbon cycle, and additionally accounting for the effect of varying climate sensitivity from 1.5 to 4.5°C (Joos *et al.* 2001).

(A)

(B)
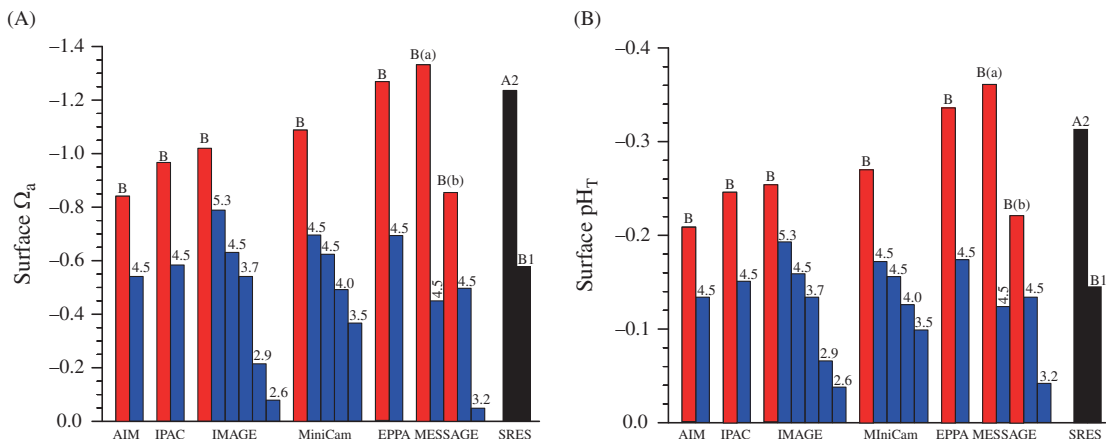
Figure 14.3 21st century change in global-mean surface saturation with respect to aragonite (Ω_a) and change in global-mean surface-ocean pH_T for the range of recent multigas mitigation (blue columns) and baseline (red, 'B') scenarios and the two illustrative SRES scenarios A2 and B1 (black). Numbers indicate the radiative forcing target in W m^{-2} associated with each mitigation scenario. The labels below the columns refer to individual IAMs or to the SRES scenarios. Results are from the standard set-up of the Bern2.5CC model.

CO_2. Ω_a decreases from a pre-industrial value of 3.7 to between 2.3 and 1.8 for the baseline scenarios and to between 3.1 and 2.4 for the mitigation scenarios using the standard model parameters. Again, uncertainties in the projections associated with the carbon cycle and climate sensitivity are largest for the high-emissions scenarios and lower-bound projected Ω_a becomes as low as a global average of 1.4 for the reference scenario with the highest emissions. Global average surface pH_T decreases from a pre-industrial value of 8.18 to 7.88–7.73 for the baseline scenarios and to 8.05–7.90 for the mitigation scenarios, with a lower bound value for the most extreme scenario of 7.6. The uncertainty ranges for Ω_a and pH_T stem almost entirely from uncertainties in the projection of atmospheric CO_2 as carbonate chemistry parameters are well defined and surface-water CO_2 follows the atmospheric rise relatively closely. Trends in surface saturation and pH_T are strongly declining in 2100 for the baseline scenarios, whereas the mitigation scenarios show small or even increasing trends.

The difference between baseline and mitigation scenarios is further highlighted by analysing the overall change in global-mean surface saturation state and pH_T over the 21st century (Fig. 14.3). Surface-ocean mean Ω_a changes over this century between –0.1 and –0.8 for the mitigation scenarios and between –0.9 and –1.4 for the baseline set.

Changes in pH_T are, with a change by –0.04 to –0.19 units, also much smaller for the mitigation than for the baseline set (–0.21 to –0.36).

The following conclusions emerge. Mitigation scenarios decisively lead to lower changes in atmospheric CO_2, to less climate change, and less ocean acidification. The difference in trends by 2100 implies that 21st century mitigation scenarios have a higher impact on the additional increase in CO_2, the additional warming, and the additional ocean acidification even beyond the 21st century than the differences between baseline and mitigation scenarios reported above for 2100. Assuming that these scenarios represent a lower bound on feasible emissions reductions, these results represent an estimate of the 'minimum warming' and of 'minimum ocean acidification' that considers inertia of both the climate system and socio-economic systems.

14.4 Inertia in the earth system: long-term commitment to ocean acidification by 21st century emissions

Simulations in which emissions of carbon and other forcing agents are hypothetically stopped in the year 2000 or 2100 allow us to investigate the legacy effects, i.e. the commitment, of historical and 21st century emissions. Three idealized 'emission-commitment' scenarios run with the NCAR

CSM1.4-carbon model have been selected to illustrate the long-term influence of anthropogenic carbon emissions on ocean acidification and climate (Fig. 14.4). In the first scenario ('Hist' case), emissions are hypothetically set to zero in 2000. In the other two scenarios, emissions follow the SRES B1 (low 'B1_c' case) and SRES A2 (high 'A2_c' case) path until 2100, when emissions are instantaneously set to zero. Setting emissions immediately to zero in 2000 or 2100 is not realistic, but it allows the quantification of the long-term impact of previous greenhouse gas emissions. The three scenarios roughly span the range of 21st century carbon emissions from baseline and mitigation scenarios (Fig. 14.2A). The 'Hist' case obviously features lower emissions (397 Gt C) than any of the mitigation scenarios. Cumulative emissions in the 'B1_c' case (1360 Gt C) are somewhat smaller than to those from the highest mitigation scenario and the lowest baseline scenario shown in Figs 14.1 and 14.2 and emissions in the 'A2_c' case (2210 Gt C) are close to those of the most extreme baseline scenario.

While projected atmospheric CO_2 and surface saturation in 2100 is similar for the Bern2.5CC
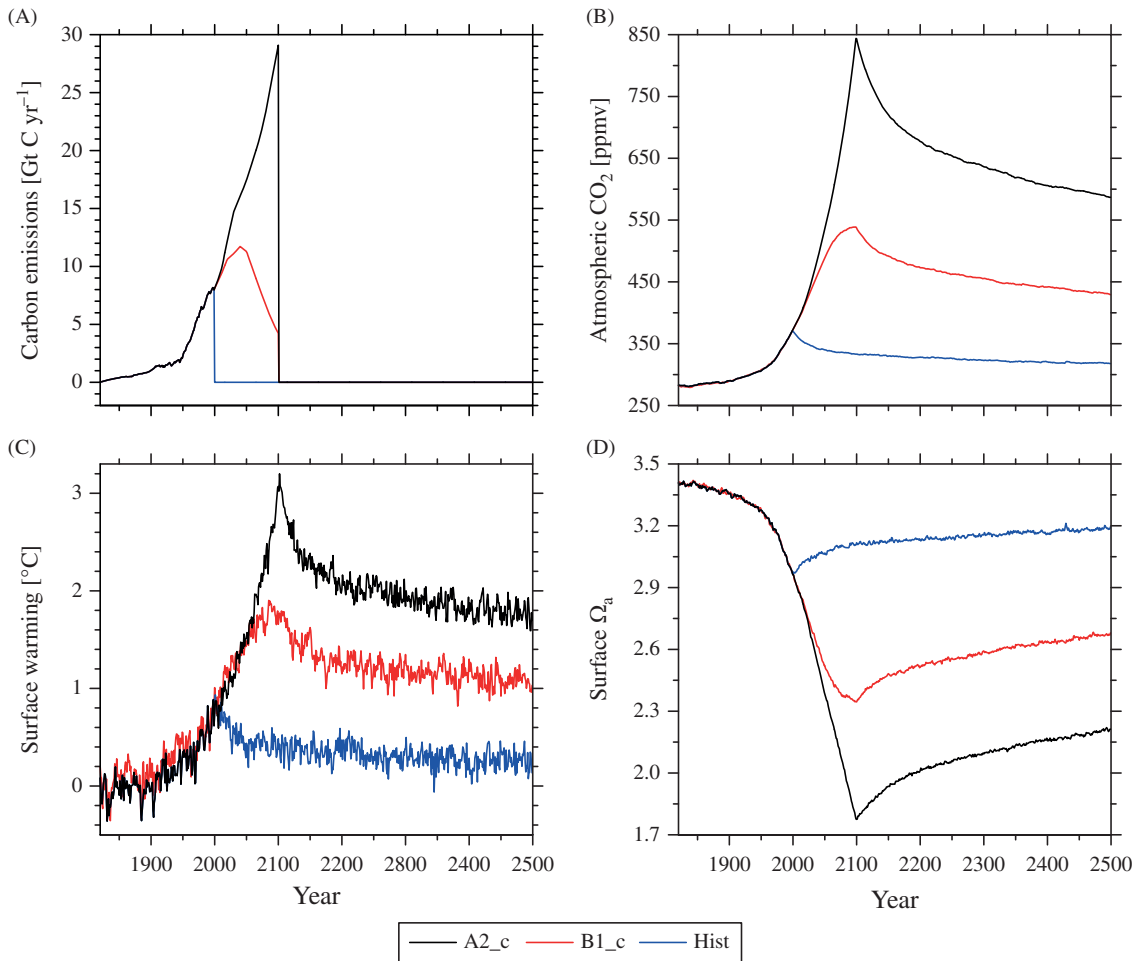
Figure 14.4   Long-term impact of 21st century carbon emissions. (A) Carbon emissions, (B) atmospheric CO_2, (C) global-mean surface air-temperature change, and (D) global average saturation state of surface waters with respect to aragonite (Ω_a) for three illustrative emissions commitment scenarios evaluated with the NCAR CSM1.4-carbon model (Frölicher and Joos 2010). In the high 'A2_c' case and the low 'B1_c' case, 21st century emissions follow the SRES A2 and SRES B1 business-as-usual scenario, respectively. Emissions are set to zero in both cases after 2100. In the 'Hist' case, emissions are stopped in the year 2000.

model (Fig. 14.2C) and the CSM1.4-carbon (Fig. 14.4B), projected 21st century warming is lower in CSM1.4-carbon than in the Bern2.5CC model. This difference is primarily related to the difference in climate sensitivity; 2°C for a nominal doubling of CO_2 in the CSM1.4 versus 3.2°C for the Bern2.5CC best estimate.

Atmospheric CO_2 concentration increases by 300% and by 190% over this century in the high 'A2_c' and low 'B1_c' case, respectively (Fig. 14.4B). Thereafter, atmospheric CO_2 decreases only very slowly, although carbon emissions are (unrealistically) reduced to zero in 2100. Atmospheric CO_2 concentration is still twice as high by 2500 than in pre-industrial times in the 'A2_c' case. On the other hand, CO_2 falls below 350 ppmv within a few decades in the 'Hist' case. The global-mean surface temperature anomaly peaks at 3°C in the 'A2_c' case and at 1.7°C in the 'B1_c' case and remains elevated for centuries (Fig. 14.4C). In the 'Hist' case, global-mean surface temperature remains only slightly perturbed (0.2°C warming) by 2500. The global average saturation state of aragonite in the surface ocean closely follows the evolution of atmospheric CO_2. Mean surface Ω_a is reduced by about half in 2100 for the 'A2_c' case and remains reduced over the next centuries.

The long perturbation lifetime of CO_2 is a consequence of the centennial to millennial timescales of overturning of various carbon reservoirs. Most of the excess carbon is taken up by the ocean and slowly (on a multicentury to millennial timescale) mixed down to the abyss. Ultimately, interaction with ocean sediments and the weathering cycle will remove the anthropogenic carbon perturbation from the atmosphere on timescales of millennia to hundreds of millennia (Archer *et al.* 1999; see Chapter 2).

In conclusion, the results from the commitment scenarios show that the magnitude of 21st century CO_2 emissions pre-determines the range of atmospheric CO_2 concentrations, temperature, and ocean acidification for the coming centuries, at least in the absence of the large-scale deployment of a technology to remove excess CO_2 from the atmosphere. In other words, the CO_2 emitted in the next decades will perturb the physical climate system, biogeochemical cycle, and ecosystems for centuries.

14.5   Regional changes in surface ocean acidification: undersaturation in the Arctic is imminent

The impacts of climate change and ocean acidification on natural and socio-economic systems depend on local and regional changes in climate and acidification rather than on global average metrics. It is important to recognize that the global-mean metrics discussed in the previous sections lead to different changes regionally (Fig. 14.5). Fortunately, the spatial patterns of change in pH_T and surface Ω_a scale closely with atmospheric CO_2 (Figs 14.6 and 14.7). This eases the discussion of local changes for the scenario range and enables us to make inferences for local and regional changes from projected atmospheric CO_2. This section presents regional changes in the saturation state of aragonite, Ω_a, and pH_T for the three commitment scenarios introduced in the previous section and as evaluated in the NCAR CSM1.4-carbon model.

There are large regional differences in the surface saturation state for pre-industrial conditions and in its change over time (Figs 14.5 and 14.6). The surface ocean was saturated with respect to aragonite in all regions under pre-industrial conditions (Kleypas *et al.* 1999; Key *et al.* 2004; Steinacher *et al.* 2009); the lowest saturation levels are simulated in the Arctic and in the Southern Ocean, whereas surface water with saturation values above 4 can be found in the tropics.

Surface-water saturation is projected to decrease rapidly in all regions until 2100 and remains reduced for centuries for all three zero-emission commitment scenarios (Fig. 14.6). The largest ocean-surface changes are found in the tropics and subtropics for Ω_a. In the high 'A2_c' case, Ω_a in the tropics and subtropics decreases from a saturation state of more than 4 in pre-industrial times to saturation below 2.5 at the end of the 21st century. The saturation of tropical and subtropical surface waters remains below 3 until 2500. Although experimental evidence remains scarce, these projected low saturation states in combination with other stress factors such as increased temperature pose the risk of the irreversible destruction of warm-water coral reefs (Kleypas *et al.* 1999; Hoegh-Guldberg *et al.* 2007).
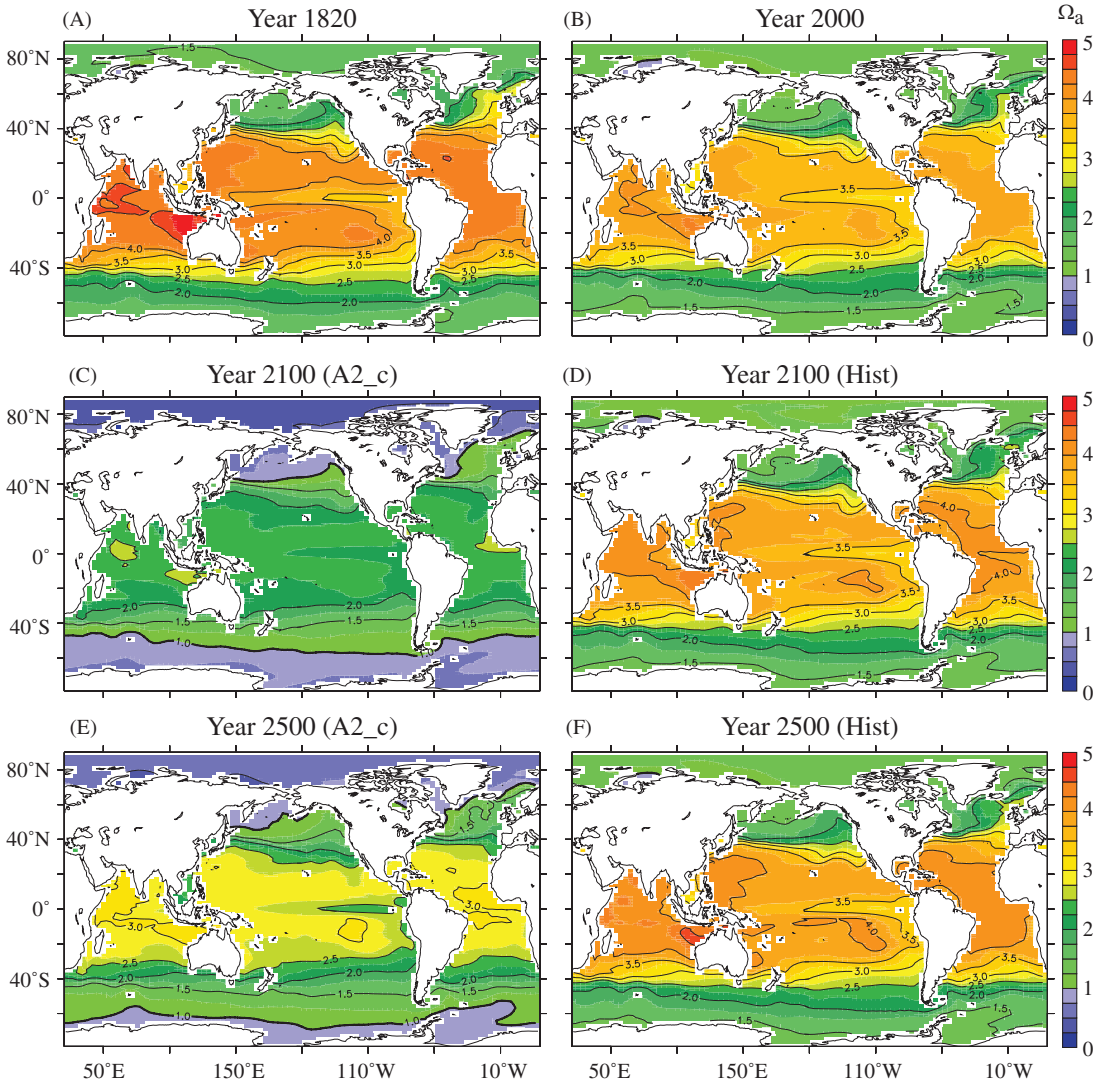
Figure 14.5 Regional distribution of the annual-mean saturation state with respect to aragonite (Ω_a) in the surface ocean for (A) pre-industrial conditions (here 1820), (B) by the year 2000, (C, D) by the end of the century, and (E, F) by 2500. The NCAR CSM1.4-carbon model was forced with reconstructed CO_2 emissions up to 2000. Emissions were set to zero after 2100 in the high 'A2_c' case (C, E) and after 2000 in the 'Hist' case (D, F). Blue colours indicate undersaturation and green to red colours supersaturation.

Undersaturation in the Arctic is imminent (Fig. 14.6C). By the time atmospheric CO_2 exceeds 490 ppmv (in 2040 in the 'A2_c' case), more than half of the Arctic Ocean will be undersaturated (annual mean; Steinacher *et al*. 2009). Undersaturation with respect to aragonite remains widespread in the Arctic Ocean for centuries even after cutting emissions in 2100 for both the 'A2_c' and the 'B1_c' cases (Frölicher and Joos 2010). The Southern Ocean

becomes undersaturated on average when atmospheric CO_2 exceeds 580 ppmv (Orr *et al.* 2005) and remains undersaturated for centuries for the 'A2_c' commitment case. Large-scale undersaturation in the Southern Ocean is avoided in the 'B1_c' and 'Hist' cases.

The main reason for the vulnerability of the Arctic Ocean is its naturally low saturation state. In addition, climate change amplifies ocean acidification in
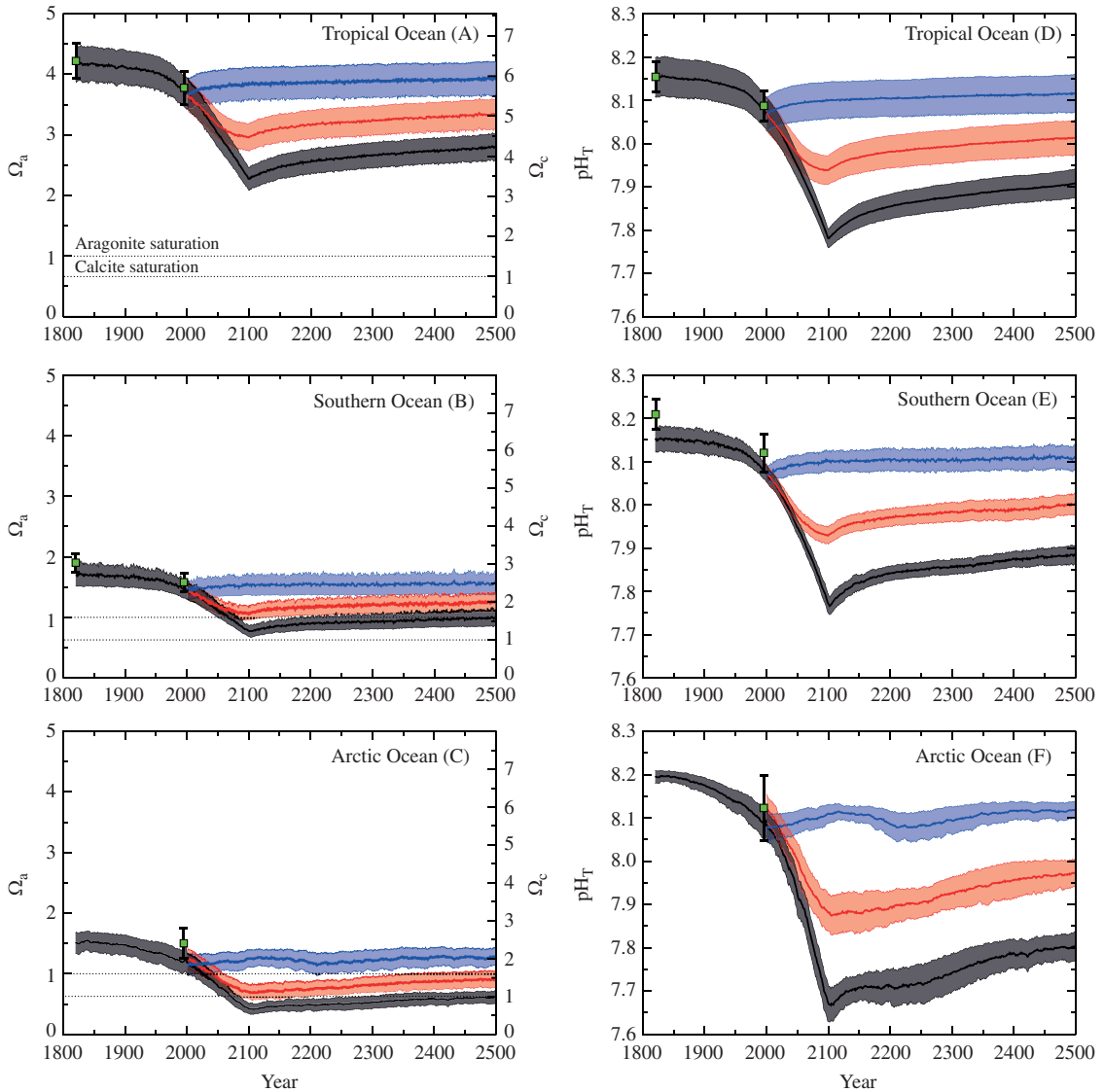
Figure 14.6 Projected evolution of CaCO$_3$ saturation states (left) and total pH (right) in the surface of the tropical ocean (30°N–30°S), Southern Ocean (60°S–90°S), and Arctic Ocean (65°N–90°N, except the Labrador and Greenland–Iceland–Norwegian seas) and for emissions commitment scenarios with no ('Hist' case, blue line, blue shading), low ('B1_c' case, red line, red shading) and high ('A2_c' case, black line, grey shading) emissions in the 21st century. Saturation with respect to aragonite, Ω_a, is indicated on the left y-axis and with respect to calcite, Ω_c, on the right y-axis. Shown are modelled annual means as well as the combined spatial and interannual variability of annual-mean values within each region (shading, ±1 SD). Observation-based estimates are shown by squares for the Southern Ocean and the tropics (GLODAP and World Ocean Atlas 2001, annual mean) and for summer conditions in the Arctic Ocean (CARINA database) with bars indicating the spatial variability. Model results are from the NCAR CSM1.4-carbon model. The level of $\Omega = 1$ separating supersaturated and undersaturated conditions for aragonite and calcite is shown by dashed, horizontal lines.
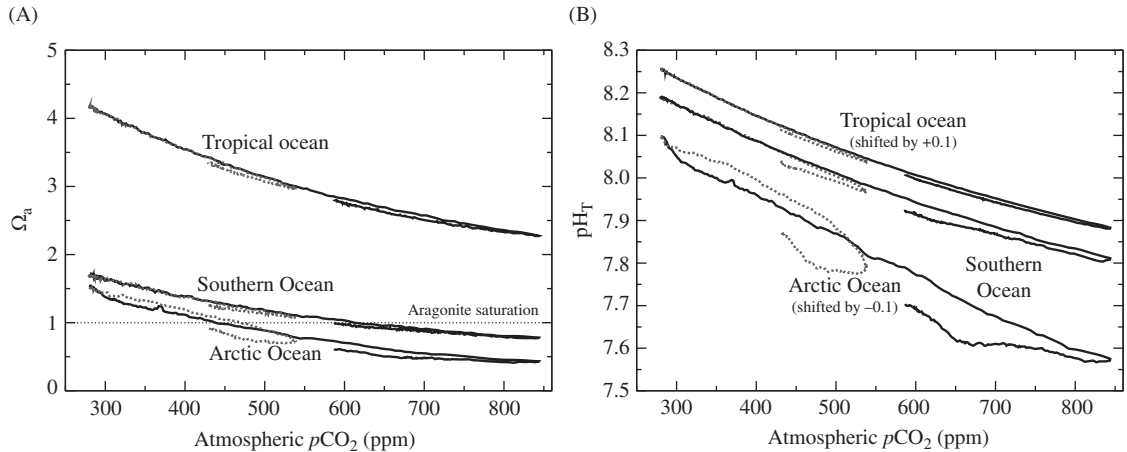
Figure 14.7   Saturation state (Ω_a) and total pH (pH_T) in surface water of three regions as a function of atmospheric CO_2. Results are from the low 'B1_c' (dashed) and high 'A2_c' (solid) commitment scenarios. The relation between atmospheric CO_2 and saturation state and pH_T shows almost no path dependency in the tropical ocean and Southern Ocean. Some path dependency is found in the Arctic Ocean, with lower values in surface saturation and pH_T for a given CO_2 concentration simulated after the peak in atmospheric CO_2. Note that the pH_T–CO_2 curves are shifted by +0.1 pH units for the tropical region and by –0.1 pH units for the Arctic region for clarity.

the Arctic, in contrast to other regions such as the Southern Ocean and the low-latitude oceans, where climate change has almost no effect on the saturation state in our simulations. Climate change amplifies the projected decrease in annual-mean Ω_a in the Arctic Ocean by 22% mainly due to surface freshening in response to the retreat of sea ice, causing local alkalinity to decrease and the uptake of anthropogenic carbon to increase (see also Chapter 3).

In summary, regional changes in the saturation state and pH_T of surface waters are distinct. The largest decrease in pH_T is simulated in the Arctic Ocean, where the lowest saturation is also found. Undersaturation is imminent in Arctic surface water (Figs 14.6 and 14.7) and remains widespread over centuries for 21st century carbon emissions of the order of 1000 Gt C or more.

14.6   Delayed responses in the deep ocean

Ocean acidification also affects the ocean interior as anthropogenic carbon continues to invade the ocean. Figure 14.8 displays how the saturation state and pH_T changes along the transect from Antarctica, through the Atlantic Ocean to the North Pole for the 'A2_c' commitment scenario. The saturation

horizon separating supersaturated from undersaturated water rises from a depth between ~2000 and 3000 m all the way up to the surface at high latitudes. The volume of water that is supersaturated with respect to aragonite strongly decreases with time. In parallel, the volume of water with low pH_T expands.

A general decrease in $CaCO_3$ saturation corresponds to a loss of volume providing habitat for many species that produce $CaCO_3$ structures. Following Steinacher *et al.* (2009), five classes of aragonite saturation levels are defined: (1) Ω_a above 4, considered optimal for the growth of warm-water corals, (2) Ω_a of 3 to 4, considered as adequate for coral growth, (3) Ω_a of 2 to 3, (4) Ω_a of 1 to 2, considered marginal to inadequate for coral growth, though experimental evidence is scarce, and finally (5) undersaturated water considered to be unsuitable for aragonite producers. Figure 14.9 shows the evolution of the ocean volume occupied by these five classes for the three commitment simulations. In the 'A2_c' case, water masses with saturation above 3 vanish by 2070 ($CO_2 \sim 630$ ppmv). Overall, the volume occupied by supersaturated water decreases from 40% in pre-industrial times to 25% in 2100 and 10% in 2300, and the volume of undersaturated water
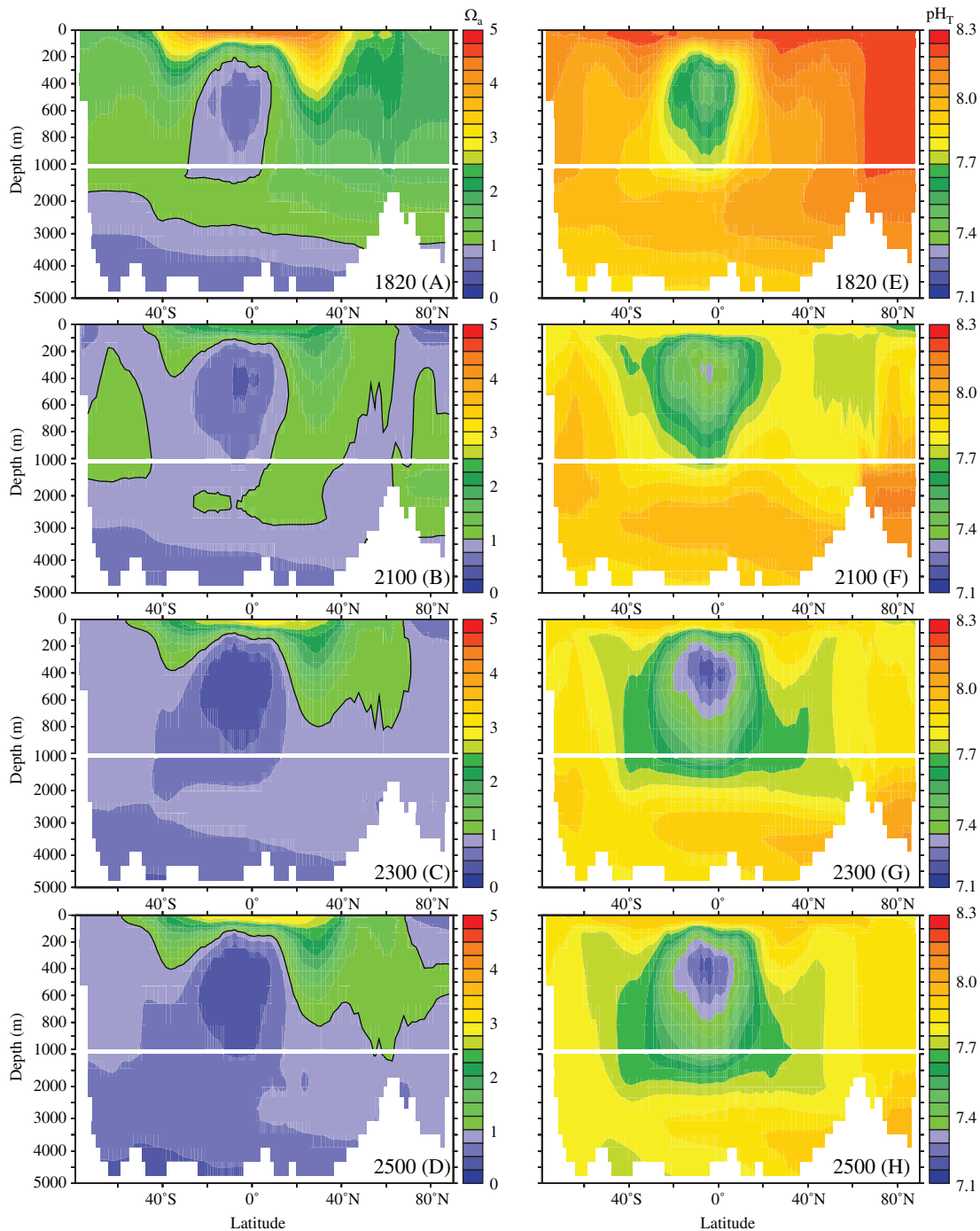
Figure 14.8   Saturation state with respect to aragonite (Ω_a, left) and total pH (pH$_T$, right) in the Atlantic and Arctic Oceans (zonal mean) for the high 'A2_c' commitment scenario by the year 1820 (A, E), 2100 (B, F), 2300 (C, G), and 2500 (D, H). Blue colours in the left panels indicate undersaturation. Note the different depth scales for the upper and the deep ocean, separated by the white horizontal line.
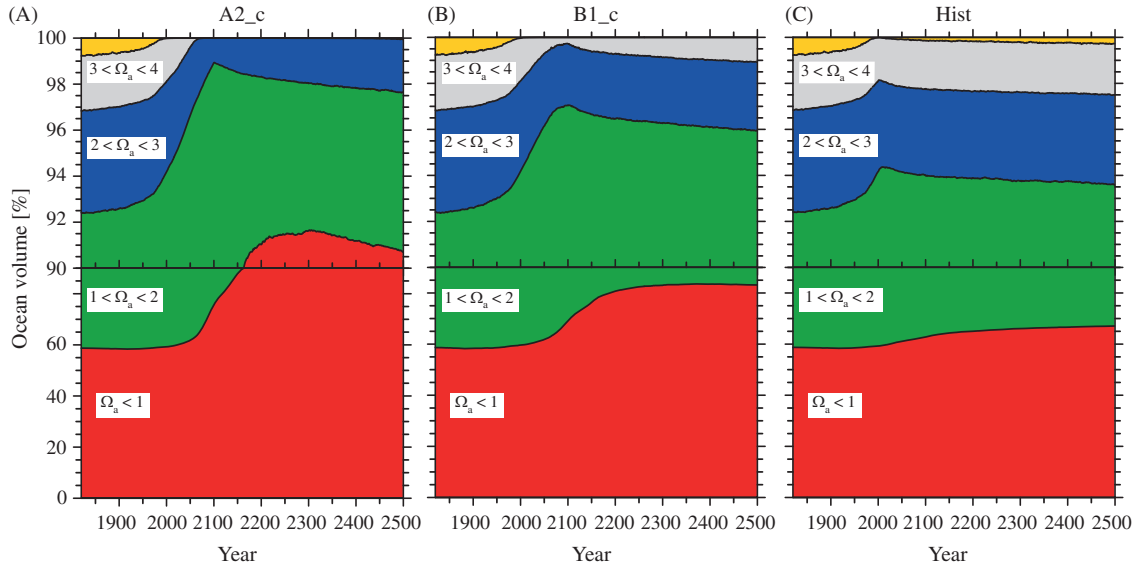
Figure 14.9   Evolution of the volume of water occupied by five classes of saturation with respect to aragonite (Ω_a) for the three illustrative emissions commitment scenarios. In the high 'A2_c' case and the low 'B1_c' case, 21st century emissions follow the SRES A2 and SRES B1 business-as-usual scenario, respectively. Emissions are set to zero in both cases after 2100. In the 'Hist' case, emissions are stopped in the year 2000. Note that the y-axis is stretched above 90%.

increases accordingly. The low 'B1_c' case also exhibits a large expansion of undersaturated water from 59 to 83% of ocean volume. In the 'Hist' case, the perturbations in volume fractions are much more modest and trends are largely reversed in the well-saturated upper ocean over the next few centuries.

The response of the saturation state is delayed in the ocean interior. This delay reflects the centennial timescales of the surface-to-deep transport of the anthropogenic carbon perturbation (Fig. 14.8). In the 'A2_c' case, the volume of undersaturated water reaches its maximum around 2300, 200 years after emissions have been stopped (Fig. 14.9). Even in the 'Hist' case, the volume fraction of supersaturated water continues to decrease. The fact that the volume fraction continues to change significantly after 2100 in the 'A2_c' and 'B1_c' cases demonstrates that some impacts of 21st century fossil fuel carbon emissions are strongly delayed and cause problems for centuries even for the extreme case of an immediate stop to emissions, i.e. the long-term commitment is substantial.

14.7   Pathways leading to stabilization of atmospheric CO$_2$

In this section, illustrative pathways leading to stabilization in atmospheric CO$_2$ are discussed in terms of their implications for projected ocean acidification and carbon emissions from the Bern2.5CC model (Fig. 14.10). The idea behind prescribing the CO$_2$ pathway is to illustrate how anthropogenic emissions have to develop if atmospheric CO$_2$ is to be stabilized as called for by the UNFCCC (UN 1992) and to illustrate the link between changes to the earth system and CO$_2$ stabilization levels.

Atmospheric CO$_2$ is prescribed to stabilize at levels ranging from 350 to 1000 ppmv. This causes surface-ocean saturation, Ω_a, to stabilize between 3.3 and 1.7 compared to a pre-industrial mean of 3.7. Surface-ocean pH$_T$ stabilizes at 8.1 to 7.7 (pre-industrial 8.2). This corresponds to an increase in the hydrogen ion concentration of 20 to 300% relative to pre-industrial times. Global-mean change of temperature of the surface ocean is between 1°C for the 350 ppmv stabilization level and 5°C for the 1000 ppmv stabilization level when the climate
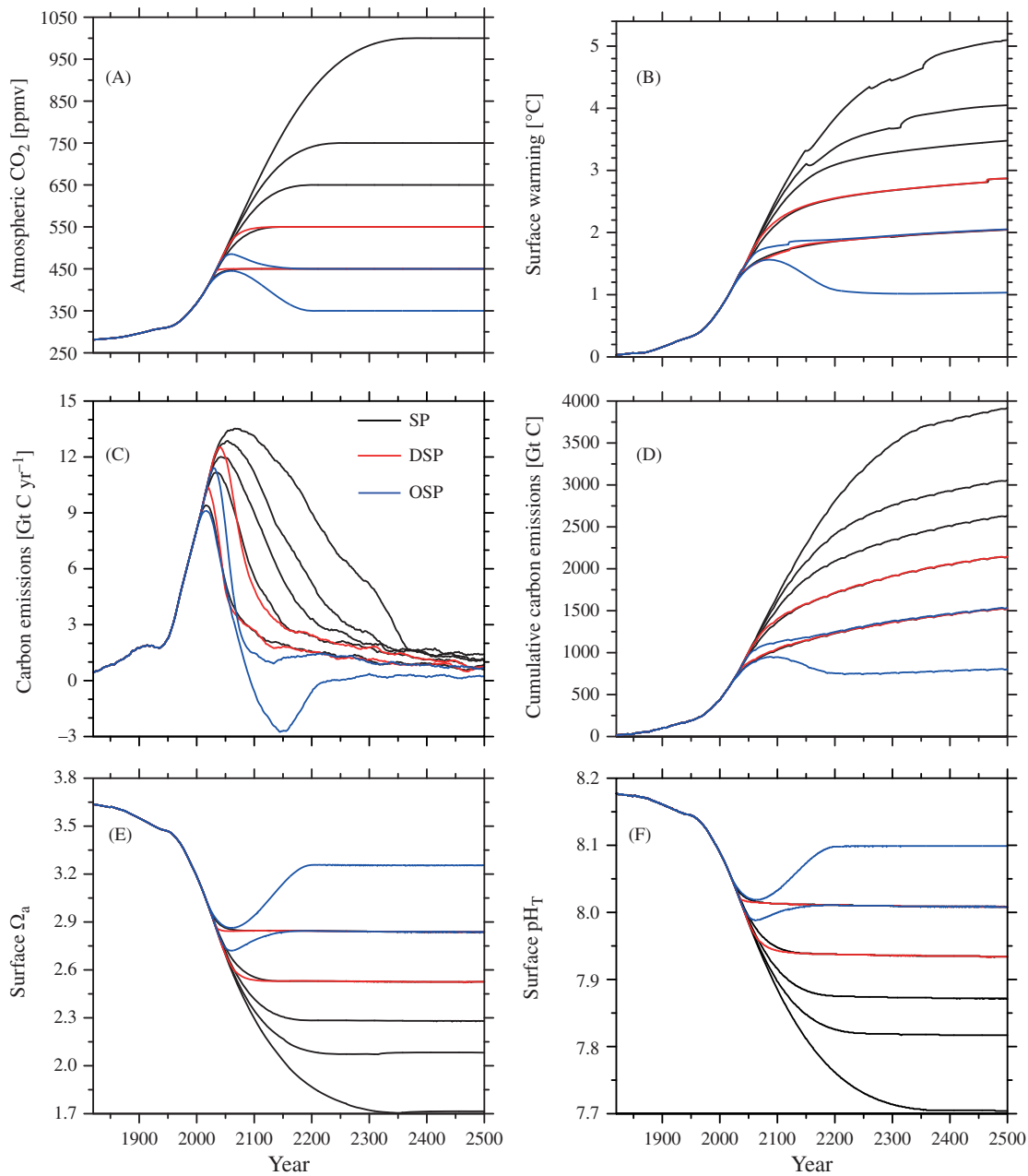
Figure 14.10 (A) Prescribed atmospheric CO_2 for pathways leading to stabilization and Bern2.5CC model projected (B) global-mean surface air temperature change, (C) annual and (D) cumulative carbon emissions, (E) global-mean surface saturation with respect to aragonite (Ω_a), and (F) global-mean surface total pH (pH_T). Pathways where atmospheric CO_2 overshoots the stabilization concentration are shown as blue lines and pathways with a delayed approach to stabilization as red lines; the different pathways to the same stabilization target illustrate how results depend on the specifics of the stabilization pathway. The label SP refers to stabilization profile, DSP to delayed stabilization profile, and OSP to overshoot stabilization profile.

sensitivity in the Bern2.5CC model is set to 3.2°C for a nominal doubling of CO_2.

Carbon emissions must drop if CO_2 is to be stabilized. Carbon emissions are allowed to increase for a few years to a few decades, depending on the pathway, but then have to drop in all cases and eventually become as low as the long-term geological carbon sink of a few tenths of a Gt C only. This is a consequence of the long lifetime of the anthropogenic perturbation. Atmospheric CO_2 thus reflects the sum of past emissions rather than current emissions. Cumulative emissions by 2500 for the Bern2.5CC model are in the range of 750 to 4000 Gt C for a stabilization between 350 and 1000 ppmv. Conventional fossil resources, mainly in the form of coal, are estimated to be about 5000 Gt C.

If emission reductions are delayed (DSP and OSP pathways in Fig. 14.10), more stringent reductions have to be implemented later in order to meet a certain stabilization target. This is illustrated by the two overshoot scenarios in which atmospheric CO_2 is prescribed to increase above the final stabilization levels and by the delayed scenarios where CO_2 is allowed to further increase initially.

The higher the emissions the larger the fraction of CO_2 emissions that stays airborne on timescales up to a few thousand years. This fraction is 20% for the 350 ppmv target and 40% for the 1000 ppmv target by the year 2500. The higher airborne fraction for high relative to low stabilization levels is primarily a consequence of the non-linearity of the seawater carbonate chemistry. The higher the partial pressure of CO_2, the smaller is the relative change in dissolved inorganic carbon for a given change in pCO_2. Thus, the partitioning of carbon between the atmosphere and the ocean shifts towards a higher fraction remaining airborne the greater the amount of carbon added to the ocean–atmosphere system.

14.8 Conclusions

We have examined a large set of projections for 21st century emissions for CO_2 and for a suite of non-CO_2 greenhouse and other air pollutant gases from the recent scenario literature (Van Vuuren *et al.* 2008b). Emissions scenarios provide an indication of the potential effects of mitigation policies. Most of the IAMs used to generate the set of baseline and

mitigation scenarios are idealized in many ways. New technologies and policies are assumed to be globally applicable and are often introduced over relatively short periods of time. Especially in the lowest mitigation scenarios, it is assumed that global climate policies can be implemented in the next few years to allow emissions to peak by 2020. These scenarios do not deal with the question of political feasibility and assume mitigation policies are implemented globally.

Physical impacts in terms of ocean acidification and climate change are lower in mitigation than baseline scenarios. Global average surface saturation with respect to aragonite is reduced to 3.1–2.4 by year 2100 in the mitigation compared to 2.3–1.8 in the baseline scenarios. The lowest scenarios result in a decrease in saturation state of 0.6 by 2100 compared with pre-industrial values and show only a small difference of 0.1 between current and end of century saturation conditions. These scenarios provide a guide to the range of global-mean surface acidification that may occur, assuming an ambitious climate policy. These low scenarios with forcing targets below 3 W m^{-2} depart from the corresponding no-climate policy baseline by 2015–2020 and incorporate the widespread development and deployment of existing carbon-neutral technologies. They require socio-political and technical conditions very different from those now existing.

Global emissions in the scenarios with a 4.5 W m^{-2} forcing target begin to diverge from baseline values by about 2020 to 2030, with emissions dropping to approximately present levels by 2100. CO_2, temperature, and ocean acidification start to diverge from the baseline projections later than emissions. This emphasizes the importance of early decisions to meet specific climate change mitigation targets.

Trends can be persistent and impacts of carbon emissions may continue for decades and centuries, long after carbon emissions have been reduced, due to the inertia in the climate–carbon system. This is exemplified by emissions commitment scenarios where carbon and other emissions are hypothetically set to zero and subsequent changes can be investigated. The projected global changes will affect different regions differently depending on their vulnerability to these changes. Widespread year-round undersaturation of surface waters in the

Arctic Ocean with respect to aragonite is likely to become reality in only a few years (Steinacher *et al.* 2009) and ocean acidification and Arctic undersaturation from baseline 21st century carbon emissions is irreversible on human timescales (Fröhlicher and Joos 2010). Globally, the volume of supersaturated water decreases for another two centuries after carbon emissions stop; the fraction of the ocean volume occupied by supersaturated water is as low as 8% in 2300 with the 'A2_c' case compared with 42% for pre-industrial conditions.

The focus of the analysis above is mainly on the magnitude of change. However, it should be stressed that rates of change are important. The rates of change of climate and ocean acidification co-determine the impacts on natural and socio-economic systems and their capabilities to adapt. Earlier analyses of the ice core and atmospheric records show that the 20th-century increase in CO_2 and its radiative forcing occurred more than an order of magnitude faster than any sustained change during at least the past 22 000 years (Joos and Spahni 2008). This implies that global climate change and ocean acidification, which are anthropogenic in origin, are progressing at high speed. It is evident from Fig. 14.2 that rates of change in surface-ocean pH_T and in Ω_a are much lower for the range of mitigation scenarios than for the range of baseline emissions scenarios.

A range of geoengineering options have been discussed to limit potential impacts of anthropogenic carbon emissions and climate change. Here, we summarize a few conclusions from a recent report (The Royal Society 2009). CO_2 removal techniques address the root cause of climate change by removing CO_2 from the atmosphere. Solar radiation management techniques attempt to offset the effects of increased greenhouse gas concentrations by causing the earth to absorb less solar radiation. Obviously, solar radiation management techniques do not contribute in a relevant way to mitigation of ocean acidification. Of the CO_2 removal methods assessed, none has yet been demonstrated to be effective at an affordable cost and with acceptable side-effects (The Royal Society 2009). If safe and low-cost methods can be deployed at an appropriate scale they could make an important contribution to reducing CO_2 concentrations and could provide a useful comple-ment to conventional emissions reductions. Methods that remove CO_2 from the atmosphere without perturbing natural systems, and without requirements for large-scale land-use changes, such as CO_2 capture from air (IPCC 2005) and possibly also enhanced weathering, are likely to have fewer side-effects. Geoengineering techniques are currently not ready for application, in contrast to low-carbon technologies.

Experimental evidence has emerged in the past years that ocean acidification has negative impacts on many organisms and may severely affect cold- and warm-water corals or high-latitude species such as aragonite-producing pteropods. Considering the precautionary principle mentioned in the UNFCCC, our results may imply that atmospheric CO_2 should be stabilized somewhere around 450 ppmv or below in order to avoid the risk of large-scale disruptions in marine ecosystems. A stabilization of atmospheric CO_2 at or below 450 ppmv requires a stringent reduction in carbon emissions over the coming decades. The results from the IAMs suggest that such a low stabilization target is economically feasible.

14.9   Acknowledgements

References

Archer, D., Kheshgi, H., and Maier-Reimer, E. (1999). Dynamics of fossil fuel CO_2 neutralization by marine $CaCO_3$. *Global Biogeochemical Cycles*, **12**, 259–76.

Brewer, P.G. and Peltzer, E.T. (2009). Limits to marine life. *Science*, **324**, 347–8.

Caldeira, K. and Wickett, M.E. (2003). Anthropogenic carbon and ocean pH. *Nature*, **425**, 365.

Cohen, A.L. and Holcomb, M. (2009). Why corals care about ocean acidification: uncovering the mechanism. *Oceanography*, **2009**, 118–27.

Comeau, S., Gorsky, G., Jeffree, R., Teyssié, J.-L., and Gattuso, J.-P. (2009). Impact of ocean acidification on a key Arctic pelagic mollusc (*Limacina helicina*). *Biogeosciences*, **6**, 1877–82.

Doney, S.C., Fabry, V.J., Feely, R.A., and Kleypas, J.A. (2009). Ocean acidification: the other CO_2 problem. *Annual Review of Marine Science*, **1**, 169–92.

Edmonds, J., Joos, F., Nakićenović, N., Richels, R.G., and Sarmiento, J.L. (2004). Scenarios, targets, gaps and costs. In: C.B. Field and M.R. Raupach (eds), *The global carbon cycle: integrating humans, climate and the natural world*, pp. 77–102. Island Press, Washington, DC.

Frank, D.C., Esper, J., Raible, C.C. *et al.* (2010). Ensemble reconstruction constraints of the global carbon cycle sensitivity to climate. *Nature*, **463**, 527–30.

Frölicher, T.L. and Joos, F. (2010). Reversible and irreversible impacts of greenhouse gas emissions in multi-century projections with the NCAR global coupled carbon cycle-climate model. *Climate Dynamics*, **35**, 1439–59.

Gangstø, R., Gehlen, M., Schneider, B., Bopp, L., Aumont, O., and Joos, F. (2008). Modeling the marine aragonite cycle: changes under rising carbon dioxide and its role in shallow water $CaCO_3$ dissolution. *Biogeosciences*, **5**, 1057–72.

Gehlen, M., Gangstø, R., Schneider, B., Bopp, L., Aumont, O., and Ethe, C. (2007). The fate of pelagic $CaCO_3$ production in a high CO_2 ocean: a model study. *Biogesciences*, **4**, 505–19.

Heinze, C. (2004). Simulating oceanic $CaCO_3$ export production in the greenhouse. *Geophysical Research Letters*, **31**, L16308, doi:10.1029/2004GL020613.

Hester, K.C., Peltzer, E.T., Kirkwood, W.J., and Brewer, P.G. (2008). Unanticipated consequences of ocean acidification: a noisier ocean at lower pH. *Geophysical Research Letters*, **35**, L19601, doi:19610.11029/12008GL034913.

Hoegh-Guldberg, O., Mumby, P.J., Hooten, A.J. *et al.* (2007). Coral reefs under rapid climate change and ocean acidification. *Science*, **318**, 1737–42.

Hutchins, D.A., Mulholland, M.R., and Fu, F. (2009). Nutrient cycles and marine microbes in a CO_2-enriched ocean. *Oceanography*, **22**, 128–45.

Iglesias-Rodriguez, M.D., Halloran, P.R., Rickaby, R.E.M. *et al.* (2008). Phytoplankton calcification in a high-CO_2 world. *Science*, **320**, 336–40.

IPCC (2005). IPCC Special Report on Carbon Dioxide Capture and Storage. Prepared by Working Group III of the Intergovernmental Panel on Climate Change (eds Metz, B., O. Davidson, H. C. de Coninck, M. Loos, and L. A. Meyer). Cambridge University Press, Cambridge.

IPCC (2007). Climate Change 2007: Mitigation. Contribution of Working Group III to the Fourth Assessment Report of the Intergovernmental Panel on Climate Change (eds B. Metz, O.R. Davidson, P.R. Bosch, R. Dave, L.A. Meyer). Cambridge University Press, Cambridge.

Joos, F. and Spahni, R. (2008). Rates of change in natural and anthropogenic radiative forcing over the past 20,000 years. *Proceedings of the National Academy of Sciences USA*, **105**, 1425–30.

Joos, F., Prentice, I.C., Sitch, S. *et al.* (2001). Global warming feedbacks on terrestrial carbon uptake under the Intergovernmental Panel on Climate Change (IPCC) emission scenarios. *Global Biogeochemical Cycles*, **15**, 891–908.

Key, R.M., Kozyr, A., Sabine, C.L. *et al.* (2004). A global ocean carbon climatology: results from Global Data Analysis Project (GLODAP). *Global Biogeochemical Cycles*, **18**, GB4031, doi:10.1029/2004GB002247.

Kleypas, J.A., Buddemeier, R.W., Archer, D., Gattuso, J.P., Langdon, C., and Opdyke, B.N. (1999). Geochemical consequences of increased atmospheric carbon dioxide on coral reefs. *Science*, **284**, 118–20.

Langdon, C. and Atkinson, M.J. (2005). Effect of elevated pCO_2 on photosynthesis and calcification of corals and interactions with seasonal change in temperature/irradiance and nutrient enrichment. *Journal of Geophysical Research – Oceans*, **110**, C09S07, doi:10.1029/2004JC002576.

Langer, G., Geisen, M., Baumann, K. *et al.* (2006). Species-specific responses of calcifying algae to changing seawater carbonate chemistry. *Geochemistry, Geophysics, Geosystems*, **7**, Q09006, doi:09010.01029/02005GC001227.

Lüthi, D., Floch, M.L., Bereiter, B. *et al.* (2008). High-resolution carbon dioxide concentration record 650,000–800,000 years before present. *Science*, **453**, 379–82.

Marland, G., Boden, T.A., and Andres, R.J. (2008). *Global, regional, and national CO_2 emissions*. Carbon Dioxide Information Analysis Center, Oak Ridge National Laboratory, US Department of Energy, Oak Ridge, TN.

Moss, R.H., Babiker, M., Brinkman, S. *et al.* (2008). *Towards new scenarios for analysis of emissions, climate change, impacts, and response strategies*, 132 pp. Intergovernmental Panel on Climate Change, Geneva.

Moss, R.H., Edmonds, J.A., Hibbard, K.A. *et al.* (2010). The next generation of scenarios for climate change research and assessment. *Nature*, **463**, 747–56.

Müller, M.N., Schulz, K.G., and Riebesell, U. (2010). Effects of long-term high CO_2 exposure on two species of coccolithophores. *Biogeosciences*, **7**, 1109–16.

Nakićenović, N. Alcamo, J., Davis, G. *et al.* (2000). *Special report on emissions scenarios*. Intergovernmental Panel on Climate Change, Cambridge University Press, New York.

Orr, J.C., Fabry, V.J., Aumont, O. *et al.* (2005). Anthropogenic ocean acidification over the twenty-first century and its impact on calcifying organisms. *Nature*, **437**, 681–6.

Plattner, G.-K., Knutti, R., Joos, F. *et al.* (2008). Long-term climate commitments projected with climate - carbon cycle models. *Journal of Climate*, **21**, 2721–51.

Schimel, D., Grubb, M., Joos, F. *et al.* (1997). *IPCC technical paper III. Stabilisation of atmospheric greenhouse gases: physical, biological, and socio-economic implications*. Inter-governmental Panel on Climate Change, Geneva.

Siegenthaler, U. and Oeschger, H. (1978). Predicting future atmospheric carbon dioxide levels. *Science*, **199**, 388–95.

Solomon, S., Qin, D., Manning, M. *et al.* (2007). Technical summary. In: S. Solomon, D. Qin, M. Manning, Z. Chen, M. Marquis, K.B. Averyt, M. Tignor, and H.L. Miller (eds), *Climate change 2007: the physical science basis. Contribution of Working Group I to the Fourth Assessment Report of the Intergovernmental Panel on Climate Change*, pp. 19–91. Cambridge University Press, Cambridge.

Steinacher, M., Joos, F., Frölicher, T.L., Plattner, G.-K., and Doney, S.C. (2009). Imminent ocean acidification in the Arctic projected with the NCAR global coupled carbon cycle-climate model. *Biogeosciences*, **6**, 515–33.

Strassmann, K.M., Joos, F., and Fischer, G. (2007). Simulating effects of land use changes on carbon fluxes: past contributions to atmospheric CO_2 increases and future commitments due to losses of terrestrial sink capacity. *Tellus B*, **60B**, 583–603.

Strassmann, K.M., Plattner, G.K., and Joos, F. (2009). CO_2 and non-CO_2 radiative forcing agents in twenty-first century climate change mitigation scenarios. *Climate Dynamics*, **33**, 737–49.

The Royal Society (2009). *Geoengineering the climate: science, governance and uncertainty*. The Royal Society, London.

UN (1992). *United Nations Framework Convention on Climate Change*. United Nations, New York.

Van Vuuren, D.P., Feddema, J., Lamarque, J.-F. *et al.* (2008a). *Work plan for data exchange between the integrated assessment and climate modeling community in support of phase-0 of scenario analysis for climate change assessment (representative community pathways)*. http://cmip-pcmdi.llnl.gov/cmip5/docs/RCP_handshake.pdf

Van Vuuren, D.P., Meinshausen, M., Plattner, G.-K. *et al.* (2008b). Temperature increase of 21st century mitigation scenarios. *Proceedings of the National Academy of Sciences USA*, **105**, 15258–62.

Weyant, J.R., de la Chesnaye, F.C., and Blanford, G.J. (2006). Overview of EMF-21: multigas mitigation and climate policy. *Energy Journal*, **27**, 1–32.